Observation of a Pomeau-Manneville intermittent route to chaos in a nonlinear oscillator

Carson Jeffries and Jose Perez
Materials and Molecular Research Division, Lawrence Berkeley Laboratory, and Department of Physics, University of California, Berkeley, California 94720
(Received 14 June 1982)

For a driven nonlinear semiconductor oscillator which shows a period-doubling pitchfork bifurcation route to chaos, we report an additional route to chaos: the Pomeau-Manneville intermittency route, characterized by a periodic (laminar) phase interrupted by bursts of aperiodic behavior. This occurs near a tangent bifurcation as the system driving parameter is reduced by ϵ from the threshold value for a periodic window. Data are presented for the dependence of the average laminar length $\langle l \rangle$ on ϵ, and also on additive random noise voltage. The results are in reasonable agreement with the intermittency theory of Hirsch, Huberman, and Scalapino. The distribution $P(l)$ is also reported.

For nonlinear dissipative systems there are many routes to chaos, i.e., patterns of behavior as the system is driven from stable smooth laminar motion into seemingly erratic or chaotic motion. In a recent review,[1] Eckmann discussed three routes, or "scenarios," that have recognizable characteristics, are reasonably well defined, and may, in fact, be considered universal; no doubt other universal routes will also be discovered, both theoretically and experimentally. In this paper we report detailed measurements on a real physical system that appears to follow one of the routes, the intermittency route originally proposed by Pomeau and Manneville (P-M).[2] Full theoretical treatments have been given by Hirsch, Huberman and Scalapino,[3] Eckmann, Thomas and Wittwer,[4] Hirsch, Nauenberg and Scalapino,[5] and Hu and Rudnick.[6] The P-M intermittency arises when a tangent bifurcation occurs and is usually modeled by a one-dimensional discrete dynamical equation of the form $x_{n+1}=f(x_n)$, where, e.g., $f(x)$ is assumed to have a single quadratic maximum, as in the logistic equation

$$x_{n+1}=\lambda x_n(1-x_n), \quad 0<\lambda\leq 4 . \tag{1}$$

As the driving parameter λ is increased from zero to $\lambda_c=3.5699\cdots$, a cascade of period-doubling pitchfork bifurcations[1,7-9] occurs with onset of aperiodicity, i.e., chaos, at the accumulation point λ_c.

In the chaotic regime $\lambda_c\leq\lambda\leq 4$, tangent bifurcations give rise to periodic windows of finite width with definite sequence and pattern—the U sequence of Metropolis, Stein, and Stein.[10]

For example, Fig. 1 is a plot of the fifth iterate $f^5(x)$ vs x for the logistic function $f(x)=\lambda(x-x^2)$ computed for $\lambda_5=3.737\,75$, where $f^5(x)$ just becomes tangent to the 45° line, giving rise to five fixed points, $x_i=f^5(x_i,\lambda_5)$, and a period-5 window. Define $\epsilon\equiv\lambda_5-\lambda$. For a small positive value of ϵ, the neighborhood of a (attracting) fixed point, Fig. 2, presents a small gap through which a trajectory must traverse, as shown by a large number of successive iterates from point A to point B, during which the system appears periodic, i.e., is in a "laminar" phase. At point B the iterates move chaoti-

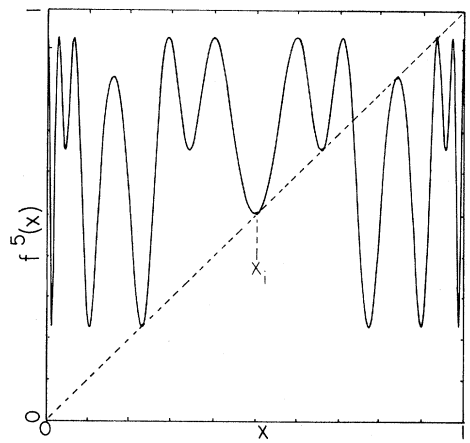

FIG. 1. The fifth iterate $f^5(x)$ vs x for the logistic $f(x)=\lambda(x-x^2)$, computed at $\lambda_5=3.737$ where five extrema of the iterate just become tangent to the 45° line. This tangent bifurcation gives rise to five stable fixed points x_i and a period-5 window.

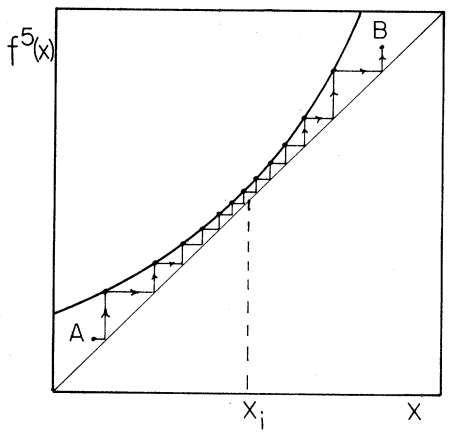

FIG. 2. An enlarged view of Fig. 1 in the neighborhood of a fixed point x_i for λ slightly less than λ_5, showing a gap. The staircase line between the iterate and the 45° line indicates successive iterations of Eq. (1). A trajectory entering at A will appear to have approximately 12 period-5 cycles of a laminar phase before it exists at B, where it displays an aperiodic burst.

cally about the map, corresponding to an intermittent "burst" phase, then reenter at some point A near some attracting fixed point, etc. To summarize, as ϵ is increased by reducing the driving parameter one expects to experimentally observe a P-M transition to chaos characterized by periodic wave trains increasingly intermittently interrupted by aperiodic bursts. The average periodic length $\langle l \rangle$ decreases with ϵ with scaling behavior[2,3]

$$\langle l \rangle \propto \epsilon^{-0.5} \tag{2}$$

for Eq. (1), or more generally, as $\langle l \rangle \propto 1/\epsilon^{1-1/Z}$ for an expansion of the iterate about the point of tangency of the form $=x+a\,|\,x\,|^{Z}$ [$Z=2$ for Eq. (1)]. For $\epsilon=0$, the P-M scenario can be induced by additive random noise, represented by adding a term $g\xi(t)$ to the right side of Eq. (1) where $\xi(t)$ is a white noise source and g is the standard deviation. The predicted[3] scaling behavior is

$$\langle l \rangle \propto g^{-2/3} \tag{3}$$

for $Z=2$, and more generally, $\langle l \rangle \propto g^{-2(Z-1)/(Z+1)}$. The probability distribution $P(l)$ is also predicted, with and without additive noise. Although onset of chaos via some kind of intermittency has been qualitatively observed in many nonlinear systems, detailed measurements demonstrating Eqs. (2) and (3) have not been yet reported to our knowledge. However, Pomeau *et al.*[11] interpret an intermittency in a chemical oscillator as belonging to this class.

We report here the observation of a P-M intermittency route to chaos in reasonable agreement with Eqs. (2) and (3) for a driven oscillator whose nonlinearity is a *p-n* junction diode, similar to that previously reported.[12] We have shown that this system follows the universal period-doubling bifurcation route to chaos.[7–9] Good agreement is found between theory and measurements for five universal numbers: convergence rate δ,[12] pitchfork ratio α,[13] power spectral ratio,[12] wide band noise scaling factor β,[13] and noise sensitivity factor κ.[14] Almost all observed window periods and patterns agree with the U sequence.[15] The bifurcation diagram is quite similar to that of Eq. (1).[12] These data characterize the system fairly well: to a good approximation it is describable by Eq. (1). However, direct observation of the return map and the Poincare section, which are more sensitive probes of the system dynamics, reveals a Henon-type two-dimensional character,[16] expected for the second-order differential equation for the LRC oscillator; this approaches the one-dimensional map as $R\rightarrow\infty$. To this approximation we consider the system to be a good candidate for observation of the P-M intermittency route, in addition to the period-doubling route.

The system is a series connected inductance L, resistance R, and junction diode, driven by an oscillator $V_0\sin(2\pi t/T)$, where the period $T=(80\text{ kHz})^{-1}=12.5\ \mu$sec, selected to be near the natural resonance period of the LRC circuit. The nonlinearity is provided by the diode which has nonlinear conductance and capacitance, both in forward and in reverse bias.[17] To take measurements on the system, we do real time analysis of the series current $I(t)$ and the voltage $V_c(t)$ across the diode. To a first approximation we assume that the system dynamical variable is the diode voltage $V_c(t)$ and make the correspondences

$$V_c(t)\leftrightarrow x_n\ ,$$

$$V_c(t+mT)\leftrightarrow x_{n+m}\ ,$$

and $|\,V_0\,|\leftrightarrow\lambda$, to relate measured quantities with x_n and λ of Eq. (1). Alternatively, we can also assume the series current $I(t)$ is the dynamical variable with the correspondences

$$I(t)\leftrightarrow x_n,\ I(t+mT)\leftrightarrow x_{n+m}$$

and $|\,V_0\,|\leftrightarrow\lambda$. Both assumptions are reasonable because V_c and I each show essentially the same bifurcation diagram, both very similar to that computed from Eq. (1). By using a sample and hold circuit and oscilloscope intensity strobing, we plot directly

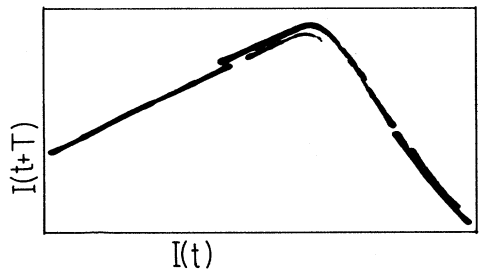

FIG. 3. Observed current $I(t+T)$ vs $I(t)$ for the nonlinear oscillator at λ slightly less than $\lambda_3=3.828$ (threshold for period-3 window), where T is the period of the driving oscillator. This corresponds to a plot of the first iterate $f(x)$ vs x and shows, to a first approximation, a single maximum. The faint splitting is due to some higher-dimensional character.

the first iterate, or return map, $I(t+T)$ vs $I(t)$, Fig. 3, which corresponds to the map x_{n+1} vs x_n. Although it is not the simple parabola of Eq. (1), to first approximation it has a single quadratic maximum; the small splitting is a consequence of higher-dimensional character.

The period-3 window has a measurable hysteresis[12] (a consequence of higher-dimensional character), and the P-M intermittency is not observable at this window. However, the first period-5 window has no observable hysteresis and displays an intermittency as λ is decreased from the periodic to the chaotic state. Figure 4(b) shows the observed fifth iterate for this window at λ chosen very slightly less than $\lambda_5=3.737$ at the start of intermittency, so that the five stable fixed points of Fig. 1 are all visited

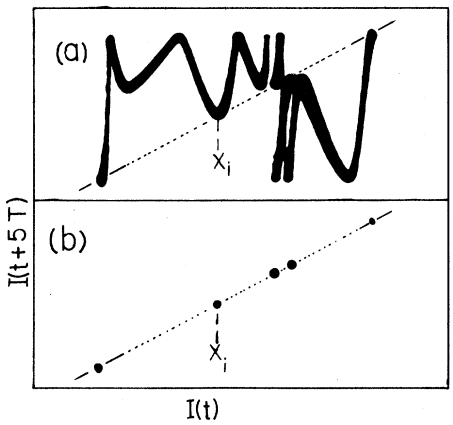

FIG. 4. Oscilloscope trace of the current $I(t+5T)$ vs $I(t)$ corresponding to the fifth iterate $f^5(x)$ vs x, for (a) λ less than λ_5, in the chaotic regime and (b) λ very slightly less than λ_5. The five points x_i lie on the straight drawn dotted line, defined by $I(t+5T)=I(t)$, and correspond to the five fixed points x_i of Fig. 1.

and can be photographed. The points lie on the straight line

$$I(t+5T)=I(t)\ .$$

Figure 4(a) shows the observed fifth iterate for λ less than λ_5, well into the chaotic region, where the complete return map is sampled more uniformly. The points of tangency to the diagonal correspond to the fixed points of Figs. 4(b) and 1. The curve of Fig. 4(a) has a reasonable correspondence with that of Fig. 1, except for a splitting due to the higher-dimensional character. Since this splitting does not intersect the diagonal line, and the system has experimentally well defined fixed points and displays tangent bifurcation, we consider the period-5 window a suitable system for observation of a P-M intermittency.

To take quantitative data to compare to Eqs. (2) and (3) we do real time analysis of the diode voltage $V_c(t)$, shown in Fig. 5 for $\epsilon=0$. The diode forward conductance clamps the positive voltage, allowing observation of voltages pulses V_c corresponding to four of the five fixed points; the pattern of Fig. 5 is $RLRR(R)$, as expected.[10] The largest pulse of $V_c(t)$ is sampled by a window comparator, which outputs an "event" pulse P, Fig. 5, if the pulse height is within 1% of the periodic (or laminar) pulse height. The 1% window was selected to facilitate comparison with the 1% gate width used in the theory of Hirsch, Huberman, and Scalapino.[3] This is further illustrated in Fig. 6 which shows $V_c(t)$ for $\epsilon>0$, i.e., for intermittency. The dots immediately below the peaks are the event pulses recorded simultaneously with $V_c(t)$ on a dual-beam oscilloscope; they are also represented schematically by the pulse sequence $P(t)$. Additional logic circuitry detects the beginning of a periodic train and outputs a pulse B; and it detects the end of the train and outputs a pulse E.

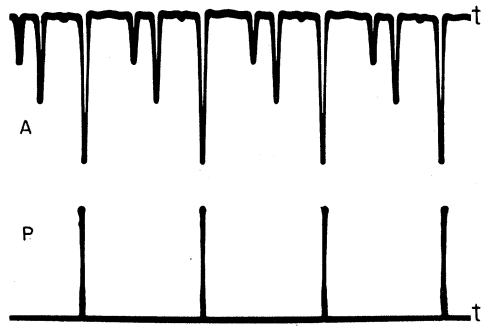

FIG. 5. Dual-beam oscilloscope trace of diode voltage $V_c(t)$ (curve A) for the period-5 window and event pulses (curve P) that detect the largest peak of $V_c(t)$. The P pulses are separated by a time $5T=62.5$ μsec.

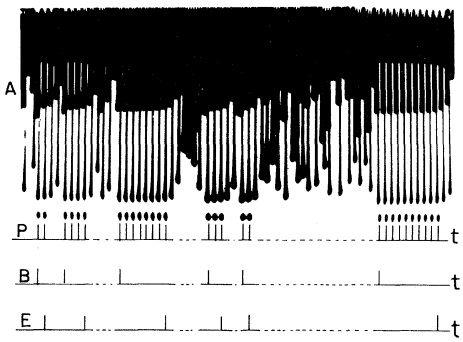

FIG. 6. Dual-beam oscilloscope trace (curve A) of $V_c(t)$ for $\epsilon \approx 10^{-3}$, showing intermittency: periodic regions (and event dots P immediately below) and aperiodic bursts. The schematically drawn pulse trains $P(t)$, $B(t)$, and $E(t)$ show, respectively, the pulses for laminar events, the beginning of a laminar region, and the end of a laminar region.

These pulses, $P(t)$, $B(t)$, and $E(t)$ are drawn schematically on Fig 6 and are the signals used to quantitatively characterize the intermittency.

Figure 7 is a representative group of intermittency signals $V_c(t)$, with event marker pulses P, shown as dots just below the periodic maxima. Here $\epsilon=0$ and the intermittency is induced by a random noise voltage V_n added to the driving voltage V_0. Figure 7(a) shows periodic trains of lengths 2, 1, 1, 2, 2, 4, and 2 (in units of $5T=62.5$ μsec). Figures 7(b) and 7(c) show longer lengths for decreasing values of V_n. We note the occurrence of some structure occasionally observed in the bursts; e.g., at region S in Fig. 7(a) there are 14 oscillations of approximately constant amplitude at period $2T$; bursts of period T and $4T$ were also occasionally observed with random amplitudes.

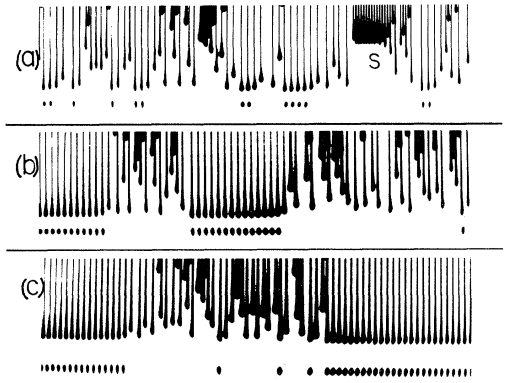

FIG. 7. A representative group of dual-beam oscilloscope traces of $V_c(t)$ as in Fig. 6 showing intermittency in the period-5 window ($\epsilon=0$), induced by a random noise voltage V_n added to the driving voltage. Traces (a), (b), and (c) correspond, respectively, to reduced values of V_n, and longer laminar lengths.

For a fast measurement of $\langle l \rangle$ we read with a two-channel frequency counter the ratio of [$f(P)$=frequency of pulses P] to [$f(B)$= frequency of pulses B]. Then, in units of $5T$ sec, the average periodic length is the frequency of periodic events divided by the frequency of periodic trains

$$\langle l \rangle = \frac{f(P)}{f(B)} . \tag{4}$$

The average length is measured as a function of ϵ, defined experimentally by

$$\epsilon = \lambda_5 - \lambda_0 = (V_{05} - V_0)\left[\frac{\Delta\lambda}{\Delta V_0}\right] , \tag{5}$$

where V_{05} is the measured driving oscillator voltage for the period 5 window threshold, and V_0 is the voltage just below threshold; a Fluke 8520A six-digit recording voltmeter was used. The scaling factor $(\Delta\lambda/\Delta V_0)$ is used to establish a measured local correspondence between V and λ in region of interest: the measurement $\Delta\lambda=\lambda_{10}-\lambda_5$ is computed from Eq. (1) where λ_{10} is the threshold for bifurcation to period 10 and ΔV_0 is the measured voltage increment between the same thresholds. For our system $(\Delta\lambda/\Delta V_0) \approx 0.103 V^{-1}$. We varied ϵ by varying V_0 by a three-stage helipot attenuator driven by a digitally controlled stepper motor with a resolution of 10^{-5} in ϵ. To record $\langle l \rangle$ vs ϵ this method was used: The P pulses were inputed into a multichannel scalar, which was advanced by one channel for every 2048 B pulses; the stepper motor then advanced to $\epsilon+\Delta\epsilon$, etc. The result is a well-averaged plot of $\langle l \rangle$ vs ϵ. A very similar procedure was used to measure $\langle l \rangle$ vs V_n, where the noise voltage V_n was slowly varied, V_0 being held fixed at $\epsilon=0$.

Figure 8 is a representative plot of $\log_{10}\langle l \rangle$ vs $\log_{10}\epsilon$. After an initial steep slope, the data are fit by $\langle l \rangle \propto 1/\epsilon^{\beta}$, where $\beta=0.43$ is the slope of the drawn line. From other similar runs an average value for the slope is found to be $\bar{\beta}=0.45\pm0.05$. The initial steep slope is not believed to be an experimental artifact. Figure 9 is a representative plot of $\log_{10}\langle l \rangle$ vs $\log_{10} g$, with $\epsilon=0$, where g is proportional to the additive noise voltage V_n. The data are fit by $\langle l \rangle \propto 1/g^{\gamma}$, where $\gamma=0.65$ is the slope of the drawn dashed line; the fit is fairly good except at large values of g. Other runs give an average value

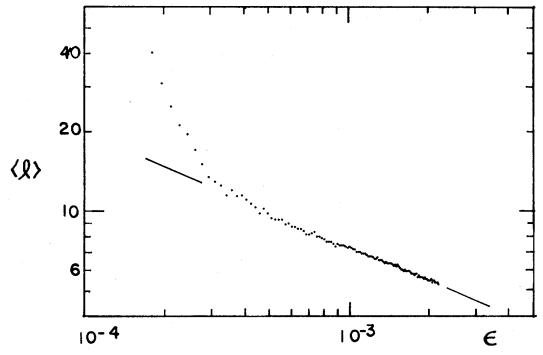

FIG 8. Points: plot of $\log_{10}\langle l\rangle$ vs $\log_{10}\langle\epsilon\rangle$ for observed intermittency near period-5 window. Dashed line through data has slope -0.43.

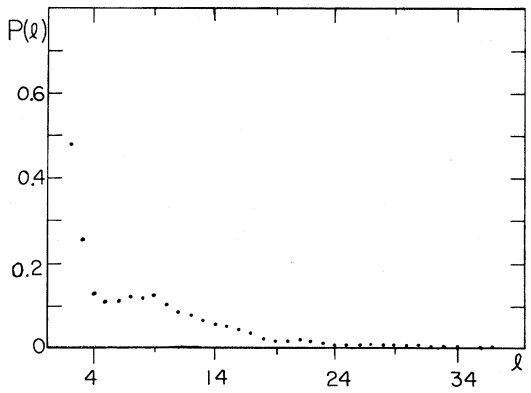

FIG. 10. Relative probability distribution $P(l)$ vs laminar length l (in units of $5T=62.5$ μsec) for intermittency near the period-5 window; $\epsilon=2.5\times10^{-4}$.

$\bar{\gamma}=0.65\pm0.05$.

A plot of the probability distribution $P(l)$ was directly measured in this way: pulse B trigged a linear ramp $V_R=K(t-t_B)$ and pulse E sampled the ramp voltage $V_R=K(t_E-t_B)$ and generated a pulse with magnitude just proportional to the length $l=t_E-t_B$; pulse E also reset V_R to zero, ready to be trigged by the next B pulse, etc. This sequence of pulses is input into a pulse height analyzer which displays directly $P(l)$ vs l. Figure 10 shows data for the unnormalized probability $P(l)$ vs l (in units of $5T=62.5$ μsec) for $\epsilon=2.5\times10^{-4}$. After an initial steep decay there is a slight hump at $l\approx9$ and then a fast fall-off to very small values of $P(l)$ for large l. Although l as large as 5000 occurred, the probability is too small to appear on Fig. 10. This figure is to be compared to the theoretical expectation (Fig. 7 of Ref. 3) which shows $P(l)$ peaked at small and large values of l with a dip at $l\approx10\approx\langle l\rangle$; however, if a small random noise voltage is added, then the computed $P(l)$ has a hump at $l\approx10$ and the peak at large l is washed out. This is qualitatively similar to our data of Fig. 10, which therefore may be explained by the presence of noise or other spurious signals in the nonlinear circuit. Data taken at $\epsilon=8\times10^{-5}$ show $P(l)$ vs l extending to $l=5000$, but with modulation at 60 Hz: at such a small value of ϵ, the intermittency is extremely sensitive to spurious amplitude modulation of the driving voltage V_0 at the power line frequency, which could not be eliminated.

The probability distribution was also measured for $\epsilon=0$ and an additive random-noise voltage of standard deviation $g=10^{-4}$ with results shown in Fig. 11; there is a very slight hump at $l\approx10$. For $g=3.5\times10^{-4}$, $P(l)$ falls off more rapidly with no hump.

To summarize, we note the reasonable correspondence between the data

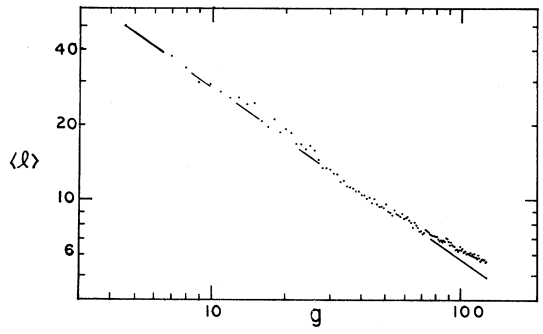

FIG. 9. Points: plot of $\log_{10}\langle l\rangle$ vs $\log_{10}$ (noise voltage) for observed intermittency in the period-5 window with $\epsilon=0$. Dashed line through data has slope -0.65.

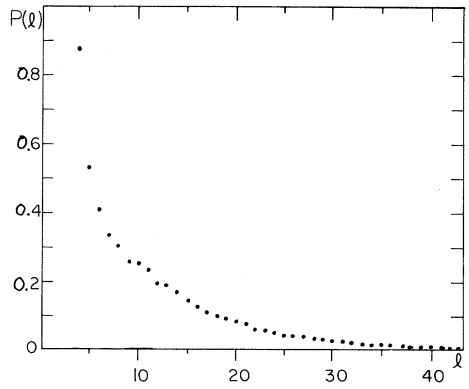

FIG. 11. Relative probability distribution $P(l)$ vs laminar length l (in units of $5T=62.5$ μsec) for intermittency in the period-5 window ($\epsilon=0$), induced by an additive random noise voltage with standard deviation $g=10^{-4}$.

$$\langle l \rangle \propto \epsilon^{-(0.45\pm0.05)} \tag{6}$$

and

$$\langle l \rangle \propto g^{-(0.65\pm0.05)} , \tag{7}$$

and the predictions of Eqs. (2) and (3). Furthermore, the observed distributions $P(l)$ vs ϵ and $P(l)$ vs g are qualitatively similar to theoretical expectation. We have no ready explanation of the small consistent deviation from $\epsilon^{-0.5}$ of the observed scaling of $\langle l \rangle$ with ϵ. The initial steep decay of $\langle l \rangle$ with ϵ (Fig. 8) and the absence of a second peak at large l in the probability distribution $P(l)$ (Fig. 10) could be due to a very small spurious 60-Hz component of the signal $V_c(t)$; other possible causes are an (unmeasurably) small hysteresis in the period-5 window, and higher-dimensional effects. These intermittency measurements are the most detailed to be reported and, we believe, establish the existence of a Pomeau-Manneville intermittency route to chaos in our driven nonlinear oscillator.

We thank J. E. Hirsch, B. A. Huberman, D. J. Scalapino, Roger Koch, and M. Nauenberg for helpful discussions. This work was supported by the Director, Office of Energy Research, Office of Basic Energy Sciences, Materials Sciences Division of the U. S. Department of Energy under Contract Number DE-AC03-76SF00098.

[1]J. -P. Eckmann, Rev. Mod. Phys. 53, 643 (1981).
[2]P. Manneville and Y. Pomeau, Phys. Lett. 75A, 1 (1979); Y. Pomeau and P. Manneville, Commun. Math. Phys. 74, 189 (1980) ("type 1" intermittency).
[3]J. E. Hirsch, B. A. Huberman, and D. J. Scalapino, Phys. Rev. A 25, 519 (1982).
[4]J.-P. Eckmann, L. Thomas, and P. Wittwer, J. Phys. A 14, 3153 (1981).
[5]J. E. Hirsch, M. Nauenberg, and D. J. Scalapino, Phys. Lett. 87A, 391 (1982).
[6]B. Hu and J. Rudnick, Phys. Rev. Lett. 48, 1645 (1982).
[7]R. M. May, Nature (London) 261, 459 (1976).
[8]S. Grossman and S. Thomae, Z. Naturforsch. 32a, 1353 (1977).
[9]M. J. Feigenbaum, J. Stat. Phys. 19, 25 (1978).
[10]N. Metropolis, M. L. Stein, and P. R. Stein, J. Comb. Theory, Ser. A 15, 25 (1973).
[11]Y. Pomeau, J. C. Roux, A. Rossi, S. Bachelort, and C. Vidal, J. Phys. (Paris) Lett. 42, L271 (1981).
[12]J. Testa, J. Perez, and C. Jeffries, Phys. Rev. Lett. 48, 714 (1982).
[13]J. Testa, J. Perez, and C. Jeffries, Lawrence Berkeley Laboratory Report No. 13719 (unpublished).
[14]J. Perez and C. Jeffries, Phys. Rev. B (in press).
[15]C. D. Jeffries and James Testa (unpublished).
[16]C. D. Jeffries and Jose Perez, Lawrence Berkeley Laboratory Report No. 14653 (unpublished).
[17]See, e.g., B. G. Streetman, *Solid State Electronic Devices* (Prentice Hall, New Jersey, 1972).